ORIGINAL ARTICLE

CrossMark

Reconfiguration patterns of large-scale brain networks in motor imagery

Tao Zhang[1,2] · Fei Wang[1] · Mengchen Li[1] · Fali Li[1] · Ying Tan[1] · Yangsong Zhang[1,4] · Hang Yang[1] · Bharat Biswal[1,5] · Dezhong Yao[1,3] · Peng Xu[1,3]

Abstract

Motor imagery (MI) is a multidimensional cognitive ability which recruited multiple brain networks. However, how connections and interactions are adjusted among distributed networks during MI remains unknown. To investigate these issues, we analyze the reconfiguration patterns of large-scale networks for different MI states. In our work, we explored the specific patterns of large-scale functional network organization from rest to different MI tasks using group independent component analysis (ICA), and evaluated the potential relationships between MI and the patterns of large-scale networks. The results indicate that task-related large-scale networks show the balanced relation between the within- and between-network connectivities during MI, and reveal the somatomotor network and dorsal attention network play critical roles in switching context-specific MI, and also demonstrate the change of large-scale networks organization toward effective topology could facilitate MI performance. Moreover, based on the large-scale network connectivities, we could differentiate an individual's three states (i.e., left-hand MI, right-hand MI and rest) with an 72.73% accuracy using a multi-variant pattern analysis, suggesting that the specific patterns of large-scale network can also provide potential biomarkers to predict an individual's behavior. Our findings contribute to the further understanding of the neural mechanisms underlying MI from large-scale network patterns and provide new biomarkers to predict the individual's behaviors.

Keywords Motor imagery · Large-scale network · ICA · Machine learning

✉ Bharat Biswal
bbiswal@gmail.com

✉ Peng Xu
xupeng@uestc.edu.cn

[1] MOE Key Lab for Neuroinformation, The Clinical Hospital of Chengdu Brain Science Institute, University of Electronic Science and Technology of China, #4, Section 2 of North Jianshe Road, Chengdu 610054, Sichuan, China

[2] Xihua University, Chengdu, China

[3] Center for Information in Medicine, School of Life Science and Technology, University of Electronic Science and Technology of China, Chengdu, China

[4] School of Computer Science and Technology, Southwest University of Science and Technology, Mianyang 621010, China

[5] Department of Biomedical Engineering, New Jersey Institute of Technology, Newark, NJ, USA

Introduction

Motor imagery (MI) is a multidimensional cognitive ability. It is normally defined as the mental rehearsal of actions from a first-person perspective, without any overt physical movement (Decety 1996). Many previous studies have reported that MI is beneficial to motor skill learning, stroke patient rehabilitation and brain–computer interface (BCI) control (Miller et al. 2010; McFarland and Wolpaw 2011; Chaudhary et al. 2016; Long et al. 2012a; Li et al. 2016). Although these benefits, there exists a debate on the rationale behind the application of MI, which is mainly due to the lack of the clear neural mechanism of MI (Pichiorri et al. 2015). Hence, it is urgent to probe the neural mechanism underlying MI, which will facilitate the better clarification of its related functional roles and provide the necessary neural basis for clinical and engineering applications.

Using functional magnetic resonance imaging (MRI) and electroencephalography (EEG) neuroimaging techniques, many studies have reported that MI involves multiple brain

🖄 Springer

regions/networks (Hetu et al. 2013; Halder et al. 2011). For example, based on direct neuroelectrical signals recording, Aflalo et al. (2015) and Hochberg et al. (2006) separately revealed that the posterior parietal cortex (PPC) and primary motor cortex (M1) are rich sources of MI-EEG signals for controlling external devices. In the EEG study conducted by (Blankertz et al. 2010), they found that the amplitude modulations of sensorimotor rhythm (SMR) can be controlled by subjects during MI, and can be used to predict the individual's MI-BCI performance. In a recent study, Hetu et al. (2013) conducted an activation likelihood estimation meta-analysis on MI, in which they provided quantitative cortical maps of different MI tasks and found that MI consistently recruited large brain areas in the fronto-parietal network, subcortical and cerebellar regions. Moreover, in our previous study, we found that an effective fronto-parietal attention network facilitates MI-BCI performance (Zhang et al. 2016). These studies enriched our knowledge of MI, but they mainly focused on the location of the functional brain regions that are involved in MI or the interactions among areas that confined within relatively local brain regions.

Recently, increasing number of neuroimaging researches consistently revealed that cognitive performance is not only associated with the interaction within multiple brain regions belonging to the same function sub-networks, as well as interactions between various sub-networks (Bressler and Menon 2010; Marek et al. 2015; Sporns 2014; Petersen and Sporns 2015). In a recent study, Tsvetanov et al. (2016) found that the connectivity patterns of both within and between large-scale functional networks are changed with age. MI is a multidimensional ability which can automatically influence different high-level cognitive processes such as attention and working memory (Madan and Singhal 2012). Thus, we hypothesized that MI cognitive function may be correlation with the interactions of within and between large-scale networks. Moreover, when subject switches to a new mental state, the brain will newly occupy the specific network structure to process the related information. Therefore, as an optimized organ, how the brain adjusts the network structure to adapt to the corresponding information processing is another important aspect of understanding the brain's working mechanism in certain cognition process. Studying the differences among distinct brain's cognitive states (i.e., tasks and rest) by exploring the changes among large-scale networks in these states can clarify how the brain responds to a given MI task. It is very important for understanding the neural processes of MI and developing the MI-based clinical applications such as motor rehabilitation (Pichiorri et al. 2015) and BCI systems (Chaudhary et al. 2016).

The functional connectivity (FC) and functional network connectivity (FNC) are two important indexes to assess the interactions within regions or between networks. In this study, we used a multivariate and data-driven spatial group independent component analysis (ICA) to investigate the interactions (FC and FNC) of large-scale networks in aggregated fMRI data (i.e., tasks and rest) by concatenating the temporal fMRI series in different tasks (Jafri et al. 2008; Calhoun et al. 2009). Though ICA has been mainly used to identify various spatially consistent resting state networks (RSNs) across subjects, while many studies have also demonstrated that the networks derived from tasks highly recapitulate the resting state networks (Smith et al. 2009; Calhoun et al. 2008; Arbabshirani et al. 2013). For example, Calhoun et al. (2008) found that spatial maps (SMs) modulated by both rest and tasks are highly spatially correlated, suggesting that the changes of SMs are subtle during different states. Moreover, these large-scale networks derived from ICA are less sensitive to head motion or physiological noise (cardiac pulsation or the respiratory cycle) (Damoiseaux et al. 2006). Thus, ICA is a powerful tool to explore the interactions of large-scale functional brain network.

Furthermore, the efficient identification of the brain states in MI, such as the left-, right-hand MI and resting state as well, is very significant for the online BCI controlling, and also is a challenge for neuroimaging. Many studies have recently demonstrated that functional brain connections are a powerful predictor of brain state or behavior (Tavor et al. 2016; Rosenberg et al. 2016; Smith 2015). For example, using a new connectome-based predictive model, Rosenberg et al. (2016) successfully identified the neuro-markers of sustained attention. Hein et al. (2016) also showed that the brain's functional network architecture could predict different human motivations with high accuracy. Thus, based on the patterns (i.e., connectivity strength or change) of large-scale network interactions in different brain states, we used the multi-variant pattern analysis (MVPA) to predict the three individual's brain states, which may contribute to identify the new biomarkers to differentiate MI tasks (i.e., left- or right-hand MI) and also to establish more efficient MI-BCI systems for specific applications such as motor rehabilitation and device control (Chaudhary et al. 2016; Moxon and Foffani 2015).

In the present study, the primary goal was to explore neural mechanisms underlying MI using the large-scale brain network connectivity patterns and MVPA. We were interested in probing (a) how the interactions within and between networks are affected by a specific MI task; (b) whether the changed connectivity of large-scale networks from rest to tasks could be used as potential biomarker to predict an individual's brain states.

Materials and methods

Participants

Twenty-six healthy undergraduate volunteers (9 females and 17 males; aged 22.85 ± 2.48 years; age range 19–26; 24 right-handed subjects) participated in the MRI experiment. The protocol was approved by the Institution Research Ethics Board of the University of Electronic Science and Technology of China (UESTC). All participants had no prior experience with SMR-BCI and had no central nervous system abnormalities or psychiatric illness. All participants were informed about the purpose of the study and written informed consent prior to any study procedure. Participants were paid a monetary compensation for their time and effort.

fMRI experimental procedure

At the beginning of the MRI scanning session, the subjects were familiarized with the full experiment process. Specifically, the subjects were instructed to use kinesthetic rather than visual imagery (Neuper et al. 2005). During fMRI scanning, resting state fMRI was collected followed by four scanning sessions that included left-/right-hand MI and left-/right-hand motor execution (ME), respectively. The task order of these four sessions was randomized for each subject. The details on the experimental process are described as follows. First, the subjects were instructed to focus on a yellow fixation cross in the center of the screen for 2 s to prepare for the following task. Then, the color of the yellow fixation cross turned white and a gray left (right) arrow also appeared on the screen, lasting 20 s during which time the subjects were instructed to perform motor imagery (execution). When the left (right) arrow disappeared, subjects were allowed have 18 s rest and asked to focus their attention on the gray fixation cross (Fig. 1). A total 20 trials were included in each run for each subject. In this study, only the fMRI data sets for left-hand MI and right-hand MI task were used for further analysis.

fMRI image acquisition

Imaging data were acquired from a GE 3.0T MRI scanner (GE DISCOVERY MR750, USA) with an 8-channel head coil at the Center for information in Medicine of UESTC. All functional images were acquired by a gradient recalled echo-planar imaging (EPI) sequence with TR = 2000 ms, TE = 30 ms, flip angle = 90°, matrix size = 64 × 64, field of
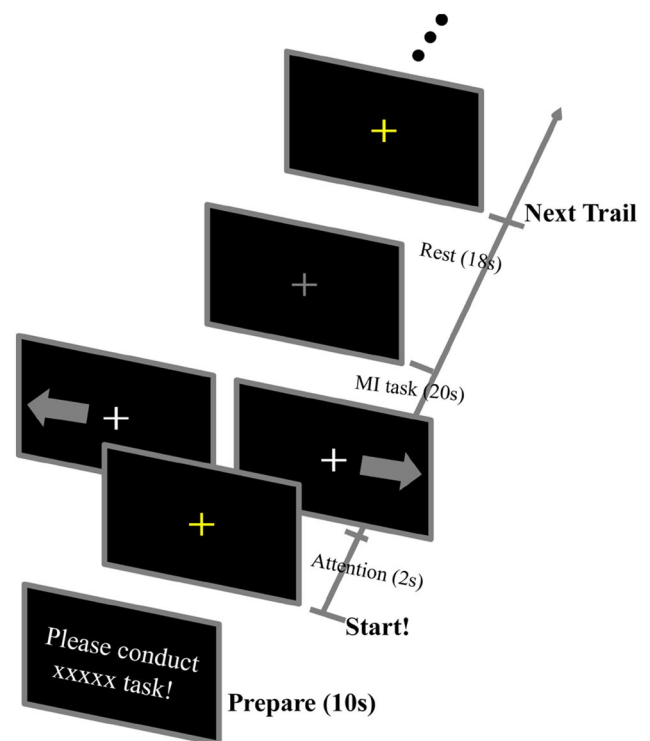

Fig. 1 MI experiment paradigm. Block design for left-/right-hand MI during MRI scanning. The 'xxxxx' denotes the description of the task such as left-hand MI or right-hand MI

view = 24 × 24 cm², slice thickness/gap = 4 mm/0.4 mm, voxel size = 3.75 × 3.75 × 4 mm³, and 32 slices oriented AC-PC line.

In the scanner, cushions and earplugs were used to reduce head movement and dampen scanner noise. Visual presentation was performed with E-prime 2.0 software (Psychology Software Tools, Inc., USA) projected onto a screen, and subjects viewed the screen via a mirror attached to the head coil. During the resting state fMRI scan, all participants were instructed to lie still with their eyes closed, relax their minds, and to not fall asleep. All participants underwent 8.5 min (255 time points) of resting state fMRI scanning. Following this resting state fMRI, the task runs were collected. Each MI task run lasted 800 s, resulting in 400 time points.

fMRI image preprocessing

The rest and tasks fMRI data sets were preprocessed in an identical fashion using the SPM8 software package (http://www.fil.ion.ucl.ac.uk/spm). First, all functional images were temporally corrected for differences in slice acquisition time. Then, the images were spatially realigned to correct for head movement artifacts. After that, the images were spatially normalized into the standard Montreal Neurological Institute (MNI) EPI space and resampled to 3 × 3 × 3 mm³

voxel resolution. Finally, all obtained images were spatially smoothed using a 6-mm full-width half-maximum (FWHM) Gaussian smoothing kernel.

Group-level ICA

Group spatial ICA was adopted to decompose the aggregated data into ICs using Gift software (version 4.0a; http://icatb.sourceforge.net/), in the following four steps: (1) data aggregation and reduction, (2) the number of component estimation, (3) group ICA decomposition, and (4) reconstruction. In step 1, before performing the group spatial ICA, we first matched the length of the time points of the MI tasks and resting state data, where the first and last 80 time points (a total of 8 trials) in the task data and the first 15 time points in resting state data were discarded, leaving 240 time points for all fMRI data. The matched data were reduced to a lower dimensionality at the subject level using principal component analysis (PCA). Then, the reduced data were concatenated together and reduced to one group. In step 2, a minimum description length (MDL) criterion was used to estimate the number of components, yielding 34 (mean MDL = 34) group components. In step 3, the entropy bound minimization (EBM) ICA algorithm (Li and Adali 2010) was utilized for components estimation, which was repeated 10 times using the minimum spanning tree (MST) (Du et al. 2014, 2016) to identify the most robust and reliable components. Finally, a GICA method was used in step 4 to reconstruct the individual subject's ICs. After reconstruction, the z-scored spatial maps and ICs' time courses were separately extracted for tasks and rest. All of the ICA components were selected by visual inspection to avoid artificial components based on previous studies (Arbabshirani et al. 2013; Mantini et al. 2009).

Group ICA based large-scale network construction

ICA method and its evolved techniques, such as subspace ICA (Sharma and Paliwal 2006) and multidimensional ICA (Cardoso 1998), are powerful tools in solving blind source separation (BSS) problems. ICA can determine a subset of spatial maximally independent components (ICs) that are known as large-scale functional networks. Approximately 20 related large-scale functional networks have been identified in the functional connectome (Menon 2011; Marek et al. 2015; Biswal et al. 2010) including the somato-motor network (SMN), the default model network (DMN) and the dorsal attention network (DAN). In addition, each IC contains an independent spatial map (SM) and its associated time course (TC) of activation (McKeown et al. 1998), where the former is expressed in terms of z scores that show the functional connectivity (FC) of given voxel TCs with the temporal signal of the specific IC (Mantini et al. 2007) and

the latter can represent a meaningful temporal dependency termed functional network connectivity (FNC) (Arbabshirani et al. 2013; Jafri et al. 2008). Thus, ICA can provide two important measures of connectivity: within-network (component) FC and between-network FNC.

In the current study, subject-specific FC spatial maps and TCs were computed for left-hand MI, right-hand MI and resting state conditions using the GICA reconstruction method. Then, within-network FC and between-network FNC were estimated using the subject-specific SMs and ICA time courses, respectively. Finally, using one-way repeated measures analysis of variance (ANOVA), significant group differences in FC and FNC across the three brain state conditions (i.e., left/right-hand MI and resting state) were highlighted. Following ANOVA analysis, post hoc paired t tests were used to determine the significant group differences in FC and FNC for the three brain states. The details for each fMRI analysis step are given in the following subsections.

Functional network connectivity

After component selection, 11 ICs were identified to be correlated with the three concerned states. Each IC was conceptualized as a specific network (Calhoun et al. 2001), which consists of multiple brain regions with a unique pattern of co-varied hemodynamic time courses. Although the components are spatially independent, temporal correlations can exist among the time courses of ICs (Jafri et al. 2008; Arbabshirani et al. 2013). We extracted the associated time courses of ICs for each subject across three states. The band-pass filter (0.01–0.1 Hz) was first performed on these time courses. Then, the Pearson's correlation of the network time courses was calculated, resulting in an 11×11 FNC matrix for each subject across three states. All correlation coefficients were transformed to a z score using a Fisher's z transform.

Statistical analysis

To compare the within-network FC and between-network FNC differences across the three states (left-hand MI, right-hand MI and resting state), we performed a one-way repeated measures analysis of variance (ANOVA) with state (tasks and rest) as a repeated measures factor. Then, paired t tests were used for post hoc testing following a significant repeated measure ANOVA. The cut-off p value for all of the tests was set at $p < 0.05$ (two-tailed) and was corrected for multiple comparisons using the false discovery rate (FDR, $p < 0.05$). The within-network FC differences were performed at the voxel-wise level using SPM8 software. For all FNC, statistical analyses were performed at functional network level after correlations were transformed to z scores using Fisher's transformation.

Networks connectivity similarity

In addition to FC and FNC, we considered the similarity of FNC pattern as a new index to measure functional network organization. In accordance with previous studies (Schultz and Cole 2016; Cole et al. 2014), we used the Pearson's correlation between the two FNC matrices to measure the similarity degree of two concerned states.

Recognition of cognitive state based on large-scale network patterns

Based on the within-network FC and between-network FNC strength, we attempted to classify an individual's three states (left-hand MI, right-hand MI and rest). We first extracted averaged within-network FC for each sub-network and an overall between-network FNC for each subject across three states. Then, an 11-dimensional FC and a 55-dimensional FNC features were obtained and used for classification. Given that some features provide minimal or redundant information for classification (Dosenbach et al. 2010). The *F* score method was employed to select features to improve the classification performance. Details of *F* score can be found in a previous study (Akay 2009; Liu et al. 2015). In the present study, support vector machine (SVM) classifier with linear and radial basis function (RBF) kernels was used. To evaluate the performance of classifier, a leave-one-out cross validation (LOOCV) strategy was adopted (Chang and Lin 2011). Regarding the optimal values for RBF kernel parameters and in the nonlinear SVM, we performed another nested LOOCV on the training set to find the corresponding optimized parameters for each training set. Then, the nonlinear SVM classifier was trained by applying the optimized parameters to the training set based on which testing set would be finally classified.

Results

Group ICA and functional network definition

From the 34 ICA components, 11 components were selected as best-fit and brain state related networks. Figure 2 shows the independent SMs of the selected networks (Figure S1 provides all 34 SMs of the components in the supplementary information). These related networks are visual networks (primary visual and extrastriate visual) (IC #1, 7, PrimVN and ExtraVN), executive control network (IC #11, ECN), default model network (IC #13, DMN), self-referential network (IC #14, SRN), frontal–parietal networks (IC #16, 20, LFPN and RFPN), salience network (IC #18, SN), somatomotor network (IC #21, SMN), dorsal attention network (IC #26, DAN), and cerebellum network (IC #28, CereN). A

detailed description of each SM including regions of activation, cluster voxels and peak activation *T* values, and MNI coordinates are provided in Supplementary Table S1.

Differences in within-network FC across three brain states

Among-group comparisons (one-way repeated measures ANOVA, $p < 0.05$, FDR corrected) showed that the ExtraVN, SMN and DAN among the 11 IC networks had significant main differences in within-network FC. Figure 3 shows that the brain regions with significant difference in these three networks included the bilateral middle occipital gyrus, right precentral gyrus and right superior frontal gyrus. Detailed information of these regions is listed in Table 1.

To determine between-group differences, we extracted the mean *z* score in the IC's spatial map across subjects using the revealed brain regions with significant among-group differences as a mask. Then, post hoc paired *t* tests were applied to these *z* scores. The statistical test revealed that the FCs of both MI task states were significantly increased compared with the resting state in ExtraVN, while no significant FC difference between left-hand MI and right-hand MI was observed in this network ($p < 0.001$; two-tailed paired *t* test; see Fig. 4a). In the SMN, left-hand MI FC was significantly increased compared to the resting state and right-hand MI, and no significant difference in FC between right-hand MI and rest was observed ($p < 0.001$; two-tailed paired *t* test; see Fig. 4b). In the DAN, the FCs of MI task states were significantly decreased compared with the resting state, and the left-hand MI FC was significantly increased compared with the right-hand MI ($p < 0.001$; two-tailed paired *t* test; see Fig. 4c).

Differences in between network FNC across three brain states

Among-group comparisons (one-way repeated measures ANOVAN, $p < 0.05$, FDR corrected) revealed the significant main differences in FNC for group, where nine-pair connections with significant differences across three states were observed (see Fig. 5a).

Based on the among-group comparison results, post hoc paired *t* tests were further applied to determine the FNC differences for each paired state (i.e., left-hand MI vs. rest, right-hand MI vs. rest, right-hand MI vs. left-hand MI) and corrected by FDR ($p < 0.05$). Compared to the FNC of resting state, we found that nine between-network edges (Fig. 5b) had significant differences in FNC during left-hand MI with five correlation pairs significantly increased (ECN-CereN, ECN-DAN, ECN-SMN, SN-DAN and SMN-DAN) and another four edges significantly decreased (extraVN-CereN, extraVN-SMN, SRN-SMN and primVN-CereN).

Fig. 2 Spatial maps of the 11 ICs of interest identified by group spatial ICA of all subjects across three states. Group maps are z-scored and voxels above a z threshold of 1 are displayed with the z score color bar denoting the different z values
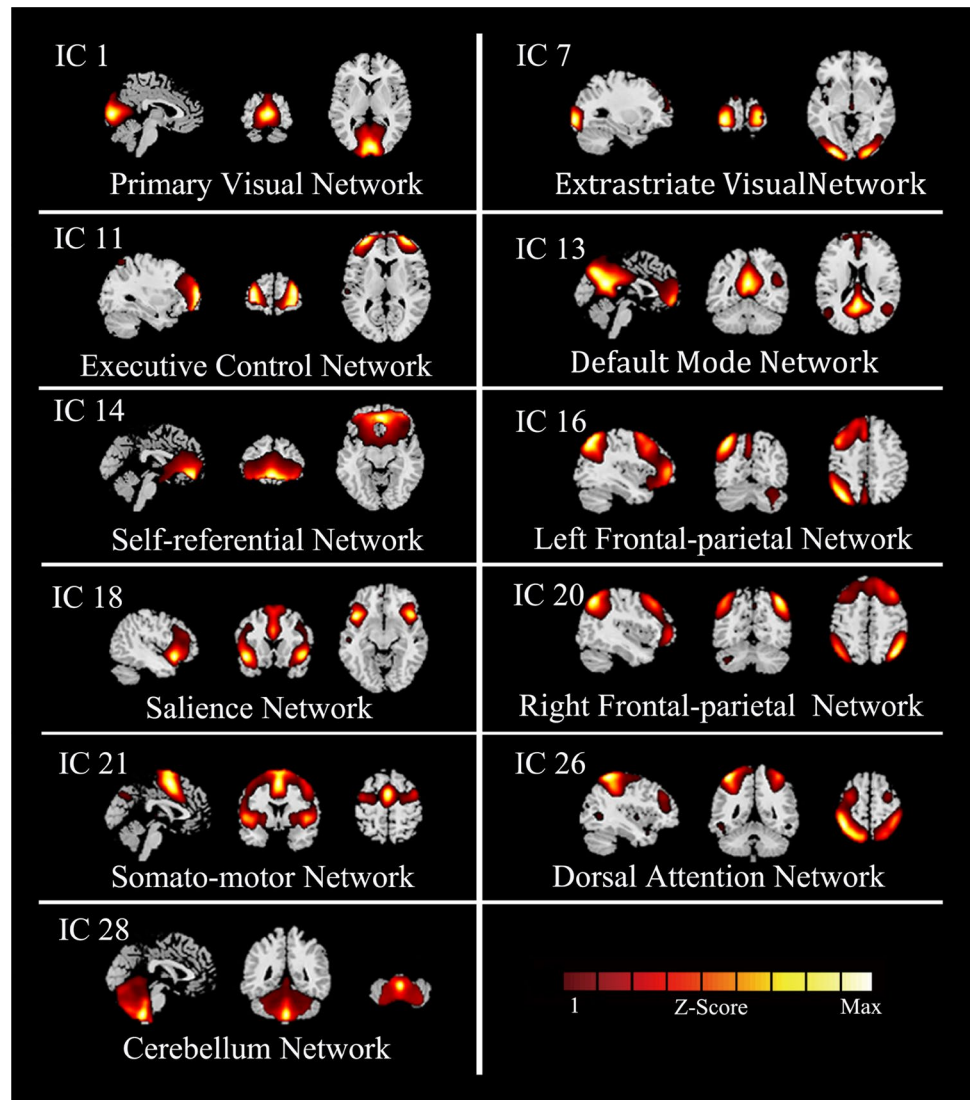
For the right-hand MI, six between-network edges (Fig. 5c) had significant differences from the resting state, of which three edges were significantly increased (ECN-CereN, ECN-SMN and SMN-DAN), while the other three edges were significantly decreased (extraVN-CereN, extraVN-SMN and SRN-SMN). For the two MI tasks, there was no significant FNC difference between left-hand MI and right-hand MI.

Network architecture is largely similar during rest and MI tasks

In the study by Cole et al. (2014), a high similarity (correlation) between FC patterns (264 nodes) during resting state and various tasks was found, revealing that task-relevant FC patterns were greatly shaped by the resting state network pattern. Similarities among FC architectures may provide new insight into better understanding MI. To further reveal the large-scale network patterns for different brain states, we

constructed FNC matrices for each subject across these three brain states. Then, the subject-specific FNC matrices were averaged according to each brain state, resulting in three FNC matrices with each corresponding to one of the three brain states. Based on the averaged FNC matrices, Pearson correlations were calculated to denote the pattern similarity between different brain states. As shown in Fig. 6, the similar adjacent matrices revealed that the three brain states had close large-scale network structures with high similarity index $r > 0.80$. The similarity index further demonstrates that the two MI tasks have more consistent network architecture with higher correlation coefficient ($r = 0.96$) compared to the resting state. These findings suggest that the patterns of the large-scale network organization during MI task only involve the adjustment of a small number of connections between networks, which also indicates that the information processing and exchange in those small numbers of networks are critical for the MI process.

Fig. 3 The main among-groups differences of within-network FC in the three states. Colors represent the values of the *F* scores which were obtained by one-way repeated measures ANOVA and corrected by FDR ($p < 0.05$)
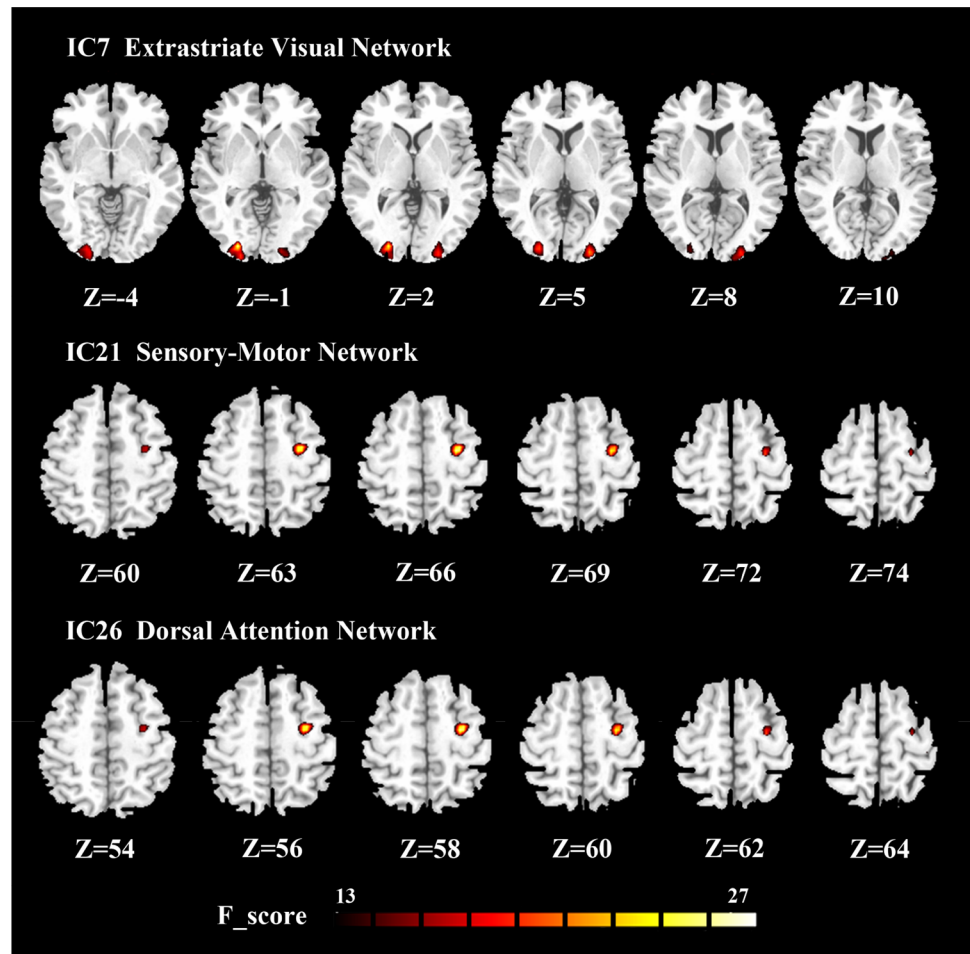

Table 1 The brain regions with significant within-network FC differences in the extraVN, SMN and DAN with a cluster size > 10 voxels

Network	Laterality	Region	BA	Peak *F* score	MNI coordinates (mm)			Cluster
					x	*y*	*z*	size
ExtraVN	L	Middle occipital gyrus	18	26.69	− 24	− 90	− 3	41
	R	Middle occipital gyrus	18	21.74	24	− 96	3	14
SMN	R	Precentral gyrus	6	27.83	27	− 24	69	33
DAN	R	Superior frontal gyrus	6	27.33	27	− 12	57	11

R right hemisphere, *L* left hemisphere

Classification results with large-scale network patterns

We take the within-network FC and between-network FNC as input for classifier, predicting an individual's cognitive state. Table 2 shows the classification results of SVM-fScore method in three feature selection conditions. Highest classification accuracy (72.73%) was obtained by concatenating the within-network FC and between-network FNC.

Discussion

In the current work, we combine multiple cognitive states (i.e., left- and right-hand MI and rest) to investigate the neural mechanisms underlying MI at large-scale network level. Using the group spatial ICA and complex brain network method, we identified the clear statistical differences in the interactions of large-scale networks during three brain states. We found that the ExtraVN, SMN and DAN were strongly modulated by MI tasks. Moreover,
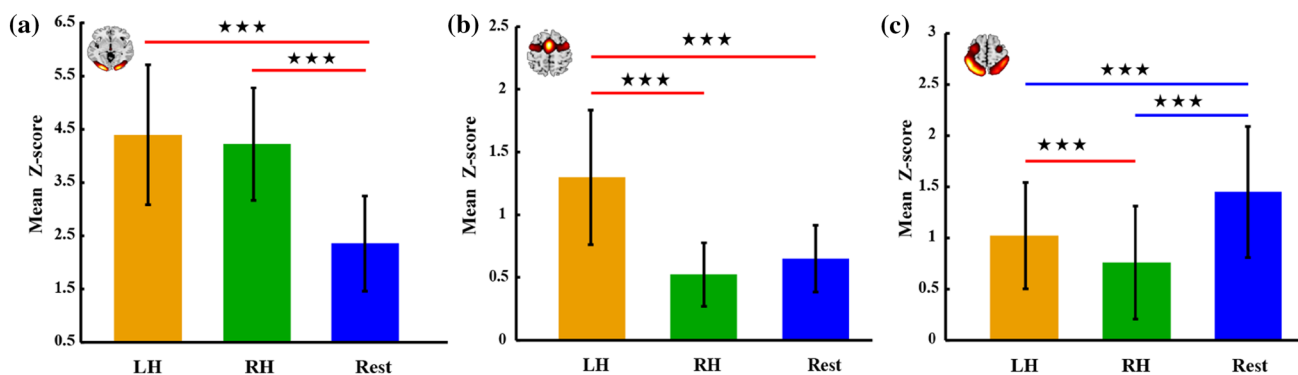
Fig. 4 The within network FC between-groups differences calculated by post hoc paired *t* tests. **a** The FC difference in the extraVN. **b** The FC differences in the SMN. **c** The FC differences in the DAN. The red line represents significantly increased FC. The blue line represents significantly decreased FC. The orange, blue and green bars represent left-hand MI, right-hand MI and resting state, respectively. LH = left-hand MI; RH = right-hand MI; 'triple stars' represents $p < 0.001$

Fig. 5 FNC differences at network level. **a** Among-group FNC differences in one-way repeated measures ANOVA tests (FDR, $p < 0.05$). The orange lines represent the *F* scores. **b** The FNC differences between left-hand MI and rest by post hoc paired *t* tests (FDR, $p < 0.05$). **c** The FNC differences between right-hand MI and rest by post hoc paired *t* test (FDR, $p < 0.05$). The red lines represent significantly increased FNC in the task compared with the resting state, and the blue lines represent significantly decreased FNC compared with the resting state. *LH* left-hand MI. *RH* right-hand MI
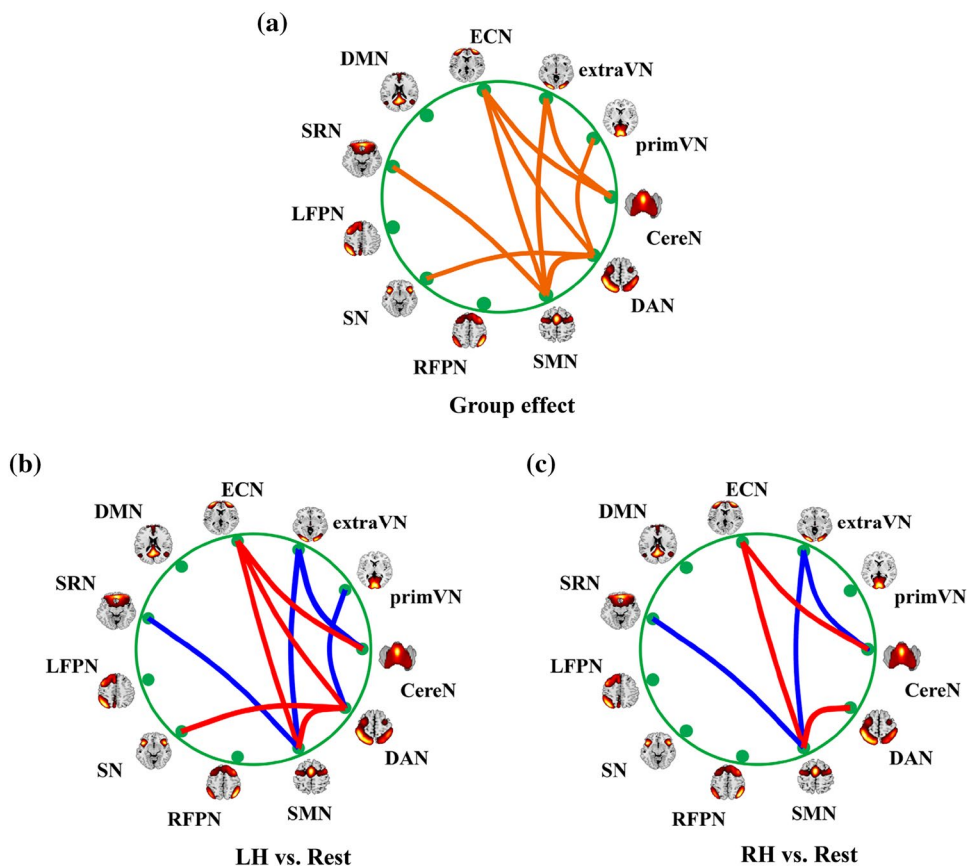
with the MVPA classification, we found that the within-network FC and between-network FNC could be used as physiological biomarkers to discriminate an individual's three cognitive states (i.e., left-/right-hand MI and rest) with high accuracy.

Differences in FC among three brain states

Within-network FC normally indicates the activation synchronization of the regions within a network. Using ANOVA analysis, we found that the FC was significantly different in

Fig. 6 Group-averaged MI task and resting state FNC matrices. **a** Left-hand MI vs. right-hand MI, **b** left-hand MI vs. resting state, **c** right-hand MI vs. resting state
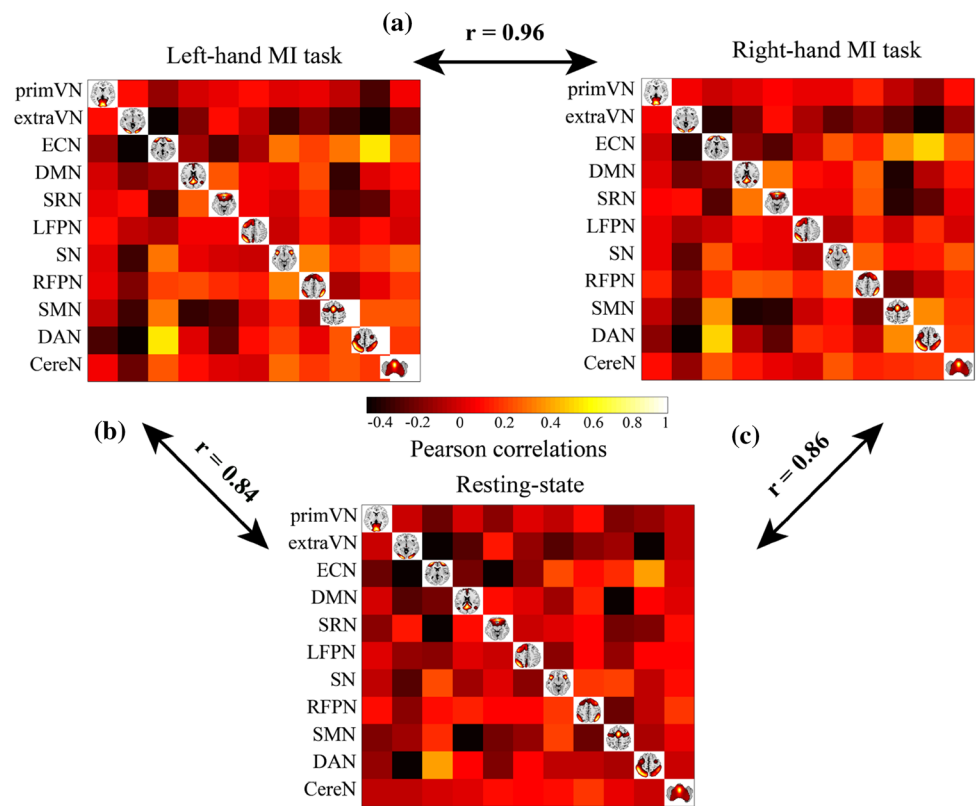

Table 2 Classification results of SVM-fScore based on large-scale network connectivity

Method	Accuracy (%)	Accuracy (%)	Accuracy (%)
Three-class	Within-network FC	Between-network FNC	FC+FNC
Non-linear SVM	59.09%	69.70%	72.73%
Linear SVM	57.58%	68.18%	71.21%

the ExtraVN, SMN and DAN among three brain states. The results implied that these three networks played important roles in MI. This is in line with the cognitive functions of these networks that consistently support externally oriented cognitions including attention, movement and spatial locations (Corbetta and Shulman 2002; Ptak and Schnider 2010; Zabelina and Andrews-Hanna 2016) and are associated with the cognitive process of MI (Moran et al. 2012; Madan and Singhal 2012).

To further explore the differences in FC for each pair of states, the post hoc paired tests were performed. For the extraVN, we found that within-network FC was significantly increased during both MI tasks as compared to rest, while there was no significant difference in FC between the left- and right-hand MI tasks (see Fig. 4a). Visual network (included primary and extrastriate networks) is a lower level sensory network, and it has an important function for receiving the sensory input (Solodkin et al. 2004). In a previous study, Hoshi and Tanji (2007) found that FC was increased in visual network in health controls compared with social

anxiety disorder (SAD) patients. Another study conducted by (Wang et al. 2015) also revealed that FC was increased in extrastriate visual network in non-drivers compared with drivers, which is due to the non-drivers need stronger brain activity to respond to the information with respect to what is possible in the forthcoming environment. In our experiment, a visual cue (i.e., a left or right arrow) was displayed on the screen to instruct the participants to perform a specific imagined hand action. The increased FC in extraVN compared with rest may account for the transformation of related visual information (i.e., cue) into the required coordinates for the corresponding MI task. There are no FC differences in extraVN between two MI-task states, which may indicate that the visual cue is less different for the two MI tasks.

For the SMN, we found that FC was significantly increased during left-hand MI compared with both rest and right-hand MI task, while there was no significant FC difference between right-hand MI and rest (see Fig. 4b). SMN is another lower-level sensory network, which consists of the primary motor cortex, premotor motor cortex

and primary sensory cortex, all of which are the key brain areas for move planning and move execution. Several previous studies have reported that MI and motor execution share common sensory and motor-related networks, and these studies also revealed that the neural activation patterns of MI are similar to that when processing real sensory and motor events (Landry et al. 2015; Gerardin et al. 2000). As all the participants were right-handed in our study, it is reasonable to speculate that left-hand MI imitates their overt counterparts stronger than right-hand MI when the participant imagines sensorimotor events (i.e., image hand movement) (Landry et al. 2015). Thus, the increased FC during left-hand MI suggests that stronger sensorimotor interactions were elicited than that of during right-hand MI. Moreover, there was no significant difference in FC between right-hand MI and rest. This indicated that a relatively low activity within SMN might contribute to prevent overt movements for the right-handed subjects.

For the DAN, the significantly decreased FC during left- and right-hand MI was observed compared to the rest (see Fig. 4c). DAN is a higher order cognitive network, which is involved in goal-oriented top-down deployment of attention (Petersen and Posner 2012). The activation of DAN is very important for indicating where, when or to what subjects should direct their attention (Hoshi and Tanji 2007). In a recent large-scale network study, Mohr et al. (2016) showed that the decreased activation in the DAN may reflect a more effective stimulus–response transformation within this network. Similar result also was found in our previous study, where we found that the reduced cortex thickness and eigenvector centrality of the brain areas within the fronto-parietal attention network were associated with MI performance (Zhang et al. 2016). MI is clearly implicated in attention and other high-level cognitive processes (Sakurada et al. 2016). We thus speculated that the decreased FC within DAN might contribute to the optimization of network resource allocation (integration of information) and also the support of other high-level cognitive functions. Interestingly, we also found that the significantly increased FC during left-hand MI compared to right-hand MI. In our study, all participants were right-handed that they are more accustomed to the right hand movement behavior. This finding may reflect that the network efficiency of DAN is higher during right-hand MI than that of left-hand MI for the right-handed subjects. In a recent study, Lewis et al. (2009) showed that a number of regions within the DAN have weaker responses during trained as compared to untrained subjects when they are learning sculpts. Thus, we suggested that the FC changes of DAN during different brain states are important for modulating the corresponding MI tasks.

Differences in FNC among three brain states

Between-network FNC primarily reflects the information interaction among large-scale networks (Marek et al. 2015), which can contribute to the understanding of the functional characteristics of cognitive functions at the network level. By comparing the between-network FNC among the three brain states, we observed the significant main group differences in FNC among nine connections (Fig. 5a). These connections are related to such sub-networks as the SN, SRN, CereN, ECN, extraVN, SMN and DAN, while no significantly different FNCs were observed for the DMN, LFPN and RFPN. These findings indicated that the related MI process was associated with the connectivity changes within networks as well as among large-scale networks.

The changes of network connectivity may be caused by the alteration in distinct task conditions. To determine the detailed changes of FNC for each pair of states, we also performed the post hoc paired tests on FNCs. By comparing with the resting state, we found nine and six paired connections had significant differences in FNC for left- and right-hand MI, where the left-hand MI involved the additional significant couplings including the DAN-ECN, DAN-SN and DAN-primVN (Fig. 5b, c). The more FNC changes during left-hand MI indicate that individuals who perform left-hand MI may need to modulate more high-level cognitive networks than right-hand MI for right-handed subjects, particularly involving the couplings from the DAN to other networks. Comparing the changed connectivity patterns in these two tasks, DAN appears to play a 'hub' role in modulating the switch between rest and task state for responding to the corresponding MI tasks. This phenomenon was also noted by Cole et al. (2013), who found that the rapid task-switching, especially in moment to moment tasks, was achieved by adjusting the functional connectivity of specific network with other networks. Thus, we suggested that the DAN tends to act as a flexible hub to switch network connectivity patterns according to the current MI task demands. In addition, based on the whole-brain network architecture, we observed that the patterns of large-scale networks were subtly modified (the number of the changes of connectivity is small) during MI tasks. Figure 5 also quantitatively shows that the MI-related FNC architecture was highly matched with that of the resting state with a similarity index above 0.84 for the three paired states. This finding is in line with previous studies (Gratton et al. 2016; Cole et al. 2014; Krienen et al. 2014), suggesting that the diverse tasks are realized by the subtle modification of the patterns of brain networks at rest.

Balanced interaction between FC and FNC during MIs

It is of interest to understand the integration and segregation of network from different scales and determine how they relate to various aspects of cognition. Combining Figs. 4 and 5, we found that an increased/decreased within-network FC is accompanied along with a decreased/increased between-network FNC during MIs, especially for the DAN, SMN and extraVN. Moreover, we computed the positive/negative changes of the FC and FNC that survived in the ANOVA analysis between task and rest, where the opposite network changes (i.e., the sum of the positive changes of FC are usually accompanied along with a sum of the negative changes of FNC for a specific network) are observed for the FC and FNC in the DAN, SMN and extraVN. Figure S2 summarized the detailed information. The converging findings in Figs. 4 and 5 and S2 consistently reveal an increased/decreased (excitatory/inhibitory) balance for the within- and between-network connectivity during MI task. Our findings are in line with previous studies, suggesting such a balance may provide a pattern that allows the brain to efficiently respond to complex external stimuli. For example, a study by Geerligs et al. (Geerligs et al. 2015) showed that the FC is decreased within the DMN and FPN, while the FNC is increased between these networks with age, which facilitated the understanding of how age affects the integration of information within and between these large-scale networks.. Thus, we suggest that MI is jointly associated with the information processing and exchange between brain regions within a network, as well as the interactions between networks, implying the interactions of networks toward collaborative network functioning (Marek et al. 2015). In the current study, we discovered a balanced interaction pattern through the change of within-network FC and between-network FNC strength during MI tasks. Indeed, this balance mainly focused on the network integration and segregation patterns at the local sub-network level. From other perspectives, Cohen et al. found that within-network communication (local and segregation) is critical for motor execution, whereas between-network communication (integrative and integration) is critical for working memory using priori ROIs and network topology properties (i.e. local efficiency, global efficiency and modularity) (Cohen and D'Esposito 2016). Using time-resolved network analysis, Shine et al. demonstrate that the human brain traverses between functional states associated with dynamic reorganization of network (i.e. maximize either segregation into tight-knit communities or integration across otherwise disparate brain regions) (Shine et al. 2016). Compared with previous studies, our findings also provide a novel insight into the optimal network structures.

Interestingly, we also found that the extraVN and DAN are modulated in opposite directions. Specifically, in MI tasks, the extraVN exhibited increased FC and decreased FNC, while the DAN showed decreased FC and increased FNC. Therefore, the connections within- and between-network showed a balanced relation between distributed and localized networks while performing an MI task, which may further infer the cooperative and competitive relationships of the related brain networks associated with MI (Deco et al. 2015).

Predicting brain's state with interaction information of large-scale network

It is important to develop special brain signatures for relevant mental processes and clinical outcomes (Woo et al. 2017; Obermeyer and Emanuel 2016). With a MVPA classification based on the large-scale network connectivity, we found that such connectivity modulated by the MI task could yield reliable classification accuracies (see Table 2). Specifically, in this study, the classification results show that the combined feature (FC + FNC) outperformed the single FC or FNC feature, where the highest 72.73% accuracy could be achieved using the kernel SVM classifier. As MI is characterized with the power decreasing in *mu* rhythm compared to the resting state EEG, the conventional way to differentiate MI task is based on the *mu* rhythm related features like the power spectrum (Kumar and Sharma 2018; Hamzah et al. 2016) and common spatial pattern features (Kumar et al. 2017; Zhang et al. 2017; Miao et al. 2017). In essence, the brain cognitive performance is largely dependent on the interactions among multiple regions as well as MI. The performed large-scale network analysis actually reveals the different network structures used by brain to process the related information in distinct MI tasks. Moreover, Figs. 4 and 5 further show that the 'switch' of states from resting to MI tasks is accomplished by the specific changes of FC and FNC. Accordingly, the combination of FC and FNC could provide the compensatory information to reliably recognize the three brain states. In practical online BCI application, besides the recognition of MI tasks, another challenging issue is the reliable detection of idle state (Li et al. 2010; Long et al. 2012b), and it is urgent to develop the efficient approach for it. Thus, MPVA analysis may provide a new strategy for the recognition of idle-state and the MI tasks using the large-scale network information.

Limitations and future work

Several methodological considerations and limitations of the current work should be considered. Although large-scale networks connectivity analysis can provide new insight into the network patterns of MI, such static network

connectivity analysis cannot capture the rapid reconfiguration and dynamic network patterns (i.e., the direction of information flow) of interactions among functional networks (Petersen and Sporns 2015). In future work, the dynamic or time-varying network connectivity analyses should be considered to better understand the instant organization patterns of the network during MI. In addition, we used the data-driven group spatial ICA to extract the within-network FC and the between-network FNC organization patterns of large-scale networks. Future studies should investigate the large-scale networks patterns of MI based on the predefined atlases such as Power regions (Power et al. 2011) and Glasser areal maps (Glasser et al. 2016). The MI-related ICs are visually selected by utilizing the prior information from the sub-network template and MI cognition process, which may be subjective and influenced by the actual operator. Considering the practical application, it is desired to utilize or develop the effective way to automatically select the task-related components.

Conclusions

Although highly recapitulated with intrinsic network, two distinct MI tasks may have different large-scale network patterns from the resting state. We constructed the structure of large-scale networks and probed the possible correlation between MI and large-scale networks. We found that FC and FNC modulation in the DAN, SMN and extraVN play important roles in switching from the resting state to the current task demand. Furthermore, combined with FC and FNC, we could predict these three brain states with high accuracy using MVPA. These findings contribute to the understanding of the underlying neural mechanisms of MI from large-scale network patterns.

Compliance with ethical standards

Conflict of interest The authors declare that they have no conflict of interest.

Ethical approval All procedures performed in this study involving human participants have been approved by the local ethics committee of the institute and are in agreement with the 1964 Helsinki declaration and its later amendments.

Informed consent All participants gave their informed consent to participate in the study.

References

Aflalo T, Kellis S, Klaes C, Lee B, Shi Y, Pejsa K, Shanfield K, Hayes-Jackson S, Aisen M, Heck C, Liu C, Andersen RA (2015) Neurophysiology. Decoding motor imagery from the posterior parietal cortex of a tetraplegic human. Science 348(6237):906–910. https://doi.org/10.1126/science.aaa5417

Akay MF (2009) Support vector machines combined with feature selection for breast cancer diagnosis. Expert Syst Appl 36(2):3240–3247. https://doi.org/10.1016/j.eswa.2008.01.009

Arbabshirani MR, Havlicek M, Kiehl KA, Pearlson GD, Calhoun VD (2013) Functional network connectivity during rest and task conditions: a comparative study. Hum Brain Mapp 34(11):2959–2971. https://doi.org/10.1002/hbm.22118

Biswal BB, Mennes M, Zuo XN, Gohel S, Kelly C, Smith SM, Beckmann CF, Adelstein JS, Buckner RL, Colcombe S, Dogonowski AM, Ernst M, Fair D, Hampson M, Hoptman MJ, Hyde JS, Kiviniemi VJ, Kotter R, Li SJ, Lin CP, Lowe MJ, Mackay C, Madden DJ, Madsen KH, Margulies DS, Mayberg HS, McMahon K, Monk CS, Mostofsky SH, Nagel BJ, Pekar JJ, Peltier SJ, Petersen SE, Riedl V, Rombouts SA, Rypma B, Schlaggar BL, Schmidt S, Seidler RD, Siegle GJ, Sorg C, Teng GJ, Veijola J, Villringer A, Walter M, Wang L, Weng XC, Whitfield-Gabrieli S, Williamson P, Windischberger C, Zang YF, Zhang HY, Castellanos FX, Milham MP (2010) Toward discovery science of human brain function. Proc Natl Acad Sci U S A 107(10):4734–4739. https://doi.org/10.1073/pnas.0911855107

Blankertz B, Sannelli C, Halder S, Hammer EM, Kubler A, Muller KR, Curio G, Dickhaus T (2010) Neurophysiological predictor of SMR-based BCI performance. NeuroImage 51(4):1303–1309. https://doi.org/10.1016/j.neuroimage.2010.03.022

Bressler SL, Menon V (2010) Large-scale brain networks in cognition: emerging methods and principles. Trends Cognit Sci 14(6):277–290. https://doi.org/10.1016/j.tics.2010.04.004

Calhoun VD, Adali T, Pearlson GD, Pekar JJ (2001) Spatial and temporal independent component analysis of functional MRI data containing a pair of task-related waveforms. Hum Brain Mapp 13(1):43–53

Calhoun VD, Kiehl KA, Pearlson GD (2008) Modulation of temporally coherent brain networks estimated using ICA at rest and during cognitive tasks. Hum Brain Mapp 29(7):828–838. https://doi.org/10.1002/hbm.20581

Calhoun VD, Liu J, Adali T (2009) A review of group ICA for fMRI data and ICA for joint inference of imaging, genetic, and ERP data. NeuroImage 45(1 Suppl):S163–S172. https://doi.org/10.1016/j.neuroimage.2008.10.057

Cardoso J-F Multidimensional independent component analysis. In: ICASSP (1998) Citeseer, pp 1941–1944

Chang CC, Lin CJ (2011) LIBSVM: a library for support vector machines. Acm T Intel Syst Technol 2 (3):27. https://doi.org/10.1145/1961189.1961199

Chaudhary U, Birbaumer N, Ramos-Murguialday A (2016) Brain–computer interfaces for communication and rehabilitation. Nat Rev Neurol 12(9):513–525. https://doi.org/10.1038/nrneurol.2016.113

Cohen JR, D'Esposito M (2016) The segregation and integration of distinct brain networks and their relationship to cognition. J Neurosci 36(48):12083–12094. https://doi.org/10.1523/JNEUROSCI.2965-15.2016

Cole MW, Reynolds JR, Power JD, Repovs G, Anticevic A, Braver TS (2013) Multi-task connectivity reveals flexible hubs for adaptive task control. Nat Neurosci 16(9):1348–1355. https://doi.org/10.1038/nn.3470

Cole MW, Bassett DS, Power JD, Braver TS, Petersen SE (2014) Intrinsic and task-evoked network architectures of the human

brain. Neuron 83(1):238–251. https://doi.org/10.1016/j.neuron.2014.05.014

Corbetta M, Shulman GL (2002) Control of goal-directed and stimulus-driven attention in the brain. Nat Rev Neurosci 3(3):201–215. https://doi.org/10.1038/nrn755

Damoiseaux JS, Rombouts SA, Barkhof F, Scheltens P, Stam CJ, Smith SM, Beckmann CF (2006) Consistent resting state networks across healthy subjects. Proc Natl Acad Sci U S A 103(37):13848–13853. https://doi.org/10.1073/pnas.0601417103

Decety J (1996) The neurophysiological basis of motor imagery. Behav Brain Res 77(1–2):45–52

Deco G, Tononi G, Boly M, Kringelbach ML (2015) Rethinking segregation and integration: contributions of whole-brain modelling. Nat Rev Neurosci 16(7):430–439. https://doi.org/10.1038/nrn3963

Dosenbach NUF, Nardos B, Cohen AL, Fair DA, Power JD, Church JA, Nelson SM, Wig GS, Vogel AC, Lessov-Schlaggar CN, Barnes KA, Dubis JW, Feczko E, Coalson RS, Pruett JR, Barch DM, Petersen SE, Schlaggar BL (2010) Prediction of individual brain maturity using fMRI. Science 329(5997):1358–1361. https://doi.org/10.1126/science.1194144

Du W, Ma S, Fu GS, Calhoun VD, Adali T (2014) A Novel Approach for Assessing Reliability of Ica for Fmri Analysis. 2014 IEEE international conference on acoustics, speech and signal processing (Icassp)

Du W, Levin-Schwartz Y, Fu GS, Ma S, Calhoun VD, Adali T (2016) The role of diversity in complex ICA algorithms for fMRI analysis. J Neurosci Methods 264:129–135. https://doi.org/10.1016/j.jneumeth.2016.03.012

Geerligs L, Renken RJ, Saliasi E, Maurits NM, Lorist MM (2015) A brain-wide study of age-related changes in functional connectivity. Cerebral Cortex 25(7):1987–1999. https://doi.org/10.1093/cercor/bhu012

Gerardin E, Sirigu A, Lehericy S, Poline JB, Gaymard B, Marsault C, Agid Y, Le Bihan D (2000) Partially overlapping neural networks for real and imagined hand movements. Cerebral cortex 10(11):1093–1104

Glasser MF, Coalson TS, Robinson EC, Hacker CD, Harwell J, Yacoub E, Ugurbil K, Andersson J, Beckmann CF, Jenkinson M, Smith SM, Van Essen DC (2016) A multi-modal parcellation of human cerebral cortex. Nature 536(7615):171–178. https://doi.org/10.1038/nature18933

Gratton C, Laumann TO, Gordon EM, Adeyemo B, Petersen SE (2016) Evidence for two independent factors that modify brain networks to meet task goals. Cell Rep 17(5):1276–1288. https://doi.org/10.1016/j.celrep.2016.10.002

Halder S, Agorastos D, Veit R, Hammer EM, Lee S, Varkuti B, Bogdan M, Rosenstiel W, Birbaumer N, Kubler A (2011) Neural mechanisms of brain–computer interface control. NeuroImage 55(4):1779–1790. https://doi.org/10.1016/j.neuroimage.2011.01.021

Hamzah N, Norhazman H, Zaini N, Sani M (2016) Classification of EEG signals based on different motor movement using multi-layer Perceptron artificial neural network. J Biol Sci 16(7):265–271

Hein G, Morishima Y, Leiberg S, Sul S, Fehr E (2016) The brain's functional network architecture reveals human motives. Science 351(6277):1074–1078. https://doi.org/10.1126/science.aac7992

Hetu S, Gregoire M, Saimpont A, Coll MP, Eugene F, Michon PE, Jackson PL (2013) The neural network of motor imagery: an ALE meta-analysis. Neurosci Biobehav Rev 37(5):930–949. https://doi.org/10.1016/j.neubiorev.2013.03.017

Hochberg LR, Serruya MD, Friehs GM, Mukand JA, Saleh M, Caplan AH, Branner A, Chen D, Penn RD, Donoghue JP (2006) Neuronal ensemble control of prosthetic devices by a human with tetraplegia. Nature 442(7099):164–171. https://doi.org/10.1038/nature04970

Hoshi E, Tanji J (2007) Distinctions between dorsal and ventral premotor areas: anatomical connectivity and functional properties. Curr Opin Neurobiol 17(2):234–242. https://doi.org/10.1016/j.conb.2007.02.003

Jafri MJ, Pearlson GD, Stevens M, Calhoun VD (2008) A method for functional network connectivity among spatially independent resting state components in schizophrenia. NeuroImage 39(4):1666–1681. https://doi.org/10.1016/j.neuroimage.2007.11.001

Krienen FM, Yeo BT, Buckner RL (2014) Reconfigurable task-dependent functional coupling modes cluster around a core functional architecture. Philos Trans R Soc Lond Ser B Biol Sci 369 (1653). https://doi.org/10.1098/rstb.2013.0526

Kumar S, Sharma A (2018) A new parameter tuning approach for enhanced motor imagery EEG signal classification. Med Biol Eng Comput:1–14

Kumar S, Mamun K, Sharma A (2017) CSP-TSM: Optimizing the performance of Riemannian tangent space mapping using common spatial pattern for MI-BCI. Comput Biol Med 91:231–242. https://doi.org/10.1016/j.compbiomed.2017.10.025

Landry SP, Page S, Shiller DM, Lepage JF, Theoret H, Champoux F (2015) Auditory imagery forces motor action. Neuroreport 26(3):101–106. https://doi.org/10.1097/WNR.0000000000000307

Lewis CM, Baldassarre A, Committeri G, Romani GL, Corbetta M (2009) Learning sculpts the spontaneous activity of the resting human brain. Proc Natl Acad Sci U S A 106(41):17558–17563. https://doi.org/10.1073/pnas.0902455106

Li XL, Adali T (2010) Independent component analysis by entropy bound minimization. IEEE Trans Signal Process 58(10):5151–5164. https://doi.org/10.1109/Tsp.2010.2055859

Li Y, Long J, Yu T, Yu Z, Wang C, Zhang H, Guan C (2010) An EEG-based BCI system for 2-D cursor control by combining Mu/Beta rhythm and P300 potential. IEEE Trans Bio-Med Eng 57(10):2495–2505

Li Y, Pan J, Long J, Yu T, Wang F, Yu Z, Wu W (2016) Multimodal BCIs: target detection, multidimensional control, and awareness evaluation in patients with disorder of consciousness. Proc IEEE 104 (2):332–352

Liu F, Guo W, Fouche JP, Wang Y, Wang W, Ding J, Zeng L, Qiu C, Gong Q, Zhang W, Chen H (2015) Multivariate classification of social anxiety disorder using whole brain functional connectivity. Brain Struct Funct 220(1):101–115. https://doi.org/10.1007/s00429-013-0641-4

Long J, Li Y, Wang H, Yu T, Pan J, Li F (2012a) A hybrid brain–computer interface to control the direction and speed of a simulated or real wheelchair. IEEE Trans Neur Syst Rehabil 20(5):720–729

Long J, Li Y, Yu T, Gu Z (2012b) Target selection with hybrid feature for BCI-based 2-D cursor control. IEEE Trans Bio-Med Eng 59(1):132–140

Madan CR, Singhal A (2012) Motor imagery and higher-level cognition: four hurdles before research can sprint forward. Cognit Process 13(3):211–229. https://doi.org/10.1007/s10339-012-0438-z

Mantini D, Perrucci MG, Del Gratta C, Romani GL, Corbetta M (2007) Electrophysiological signatures of resting state networks in the human brain. Proc Natl Acad Sci U S A 104(32):13170–13175. https://doi.org/10.1073/pnas.0700668104

Mantini D, Corbetta M, Perrucci MG, Romani GL, Del Gratta C (2009) Large-scale brain networks account for sustained and transient activity during target detection. NeuroImage 44(1):265–274. https://doi.org/10.1016/j.neuroimage.2008.08.019

Marek S, Hwang K, Foran W, Hallquist MN, Luna B (2015) The contribution of network organization and integration to the development of cognitive control. PLoS Biol 13(12):e1002328. https://doi.org/10.1371/journal.pbio.1002328

McFarland DJ, Wolpaw JR (2011) Brain–computer Interfaces for Communication and Control. Commun ACM 54(5):60–66. https://doi.org/10.1145/1941487.1941506

McKeown MJ, Makeig S, Brown GG, Jung T-P, Kindermann SS, Bell AJ, Sejnowski TJ (1998) Analysis of fMRI data by blind separation into independent spatial components

Menon V (2011) Large-scale brain networks and psychopathology: a unifying triple network model. Trends Cognit Sci 15(10):483–506. https://doi.org/10.1016/j.tics.2011.08.003

Miao M, Wang A, Liu F (2017) A spatial-frequency-temporal optimized feature sparse representation-based classification method for motor imagery eeg pattern recognition. Med Biol Eng Comput 55(9):1589–1603

Miller KJ, Schalk G, Fetz EE, den Nijs M, Ojemann JG, Rao RP (2010) Cortical activity during motor execution, motor imagery, and imagery-based online feedback. Proc Natl Acad Sci U S A 107(9):4430–4435. https://doi.org/10.1073/pnas.0913697107

Mohr H, Wolfensteller U, Betzel RF, Misic B, Sporns O, Richiardi J, Ruge H (2016) Integration and segregation of large-scale brain networks during short-term task automatization. Nat Commun 7:13217. https://doi.org/10.1038/ncomms13217

Moran A, Guillot A, Macintyre T, Collet C (2012) Re-imagining motor imagery: building bridges between cognitive neuroscience and sport psychology. Br J Psychol 103(2):224–247. https://doi.org/10.1111/j.2044-8295.2011.02068.x

Moxon KA, Foffani G (2015) Brain-Machine Interfaces beyond Neuroprosthetics. Neuron 86(1):55–67. https://doi.org/10.1016/j.neuron.2015.03.036

Neuper C, Scherer R, Reiner M, Pfurtscheller G (2005) Imagery of motor actions: differential effects of kinesthetic and visual-motor mode of imagery in single-trial EEG. Brain Res Cognit Brain Res 25(3):668–677. https://doi.org/10.1016/j.cogbrainres.2005.08.014

Obermeyer Z, Emanuel EJ (2016) Predicting the future—big data, machine learning, and clinical medicine. N Engl J Med 375(13):1216–1219. https://doi.org/10.1056/NEJMp1606181 doi

Petersen SE, Posner MI (2012) The attention system of the human brain: 20 years after. Ann Rev Neurosci 35:73–89. https://doi.org/10.1146/annurev-neuro-062111-150525

Petersen SE, Sporns O (2015) Brain networks and cognitive architectures. Neuron 88(1):207–219. https://doi.org/10.1016/j.neuron.2015.09.027

Pichiorri F, Morone G, Petti M, Toppi J, Pisotta I, Molinari M, Paolucci S, Inghilleri M, Astolfi L, Cincotti F (2015) Brain–computer interface boosts motor imagery practice during stroke recovery. Ann Neurol 77(5):851–865

Power JD, Cohen AL, Nelson SM, Wig GS, Barnes KA, Church JA, Vogel AC, Laumann TO, Miezin FM, Schlaggar BL, Petersen SE (2011) Functional network organization of the human brain. Neuron 72(4):665–678. https://doi.org/10.1016/j.neuron.2011.09.006

Ptak R, Schnider A (2010) The dorsal attention network mediates orienting toward behaviorally relevant stimuli in spatial neglect. J Neurosci 30(38):12557–12565. https://doi.org/10.1523/JNEUROSCI.2722-10.2010

Rosenberg MD, Finn ES, Scheinost D, Papademetris X, Shen X, Constable RT, Chun MM (2016) A neuromarker of sustained attention from whole-brain functional connectivity. Nat Neurosci 19(1):165–171. https://doi.org/10.1038/nn.4179

Sakurada T, Hirai M, Watanabe E (2016) Optimization of a motor learning attention-directing strategy based on an individual's motor imagery ability. Exp Brain Res Exp Hirnforschung Exp

Cerebrale 234(1):301–311. https://doi.org/10.1007/s00221-015-4464-9

Schultz DH, Cole MW (2016) Higher intelligence is associated with less task-related brain network reconfiguration. J Neurosci 36(33):8551–8561. https://doi.org/10.1523/JNEUROSCI.0358-16.2016

Sharma A, Paliwal KK (2006) Subspace independent component analysis using vector kurtosis. Pattern Recogn 39(11):2227–2232. https://doi.org/10.1016/j.patcog.2006.04.021

Shine JM, Bissett PG, Bell PT, Koyejo O, Balsters JH, Gorgolewski KJ, Moodie CA, Poldrack RA (2016) The dynamics of functional brain networks: integrated network states during cognitive task performance. Neuron 92(2):544–554. https://doi.org/10.1016/j.neuron.2016.09.018

Smith S (2015) Linking cognition to brain connectivity. Nat Neurosci 19(1):7–9. https://doi.org/10.1038/nn.4206

Smith SM, Fox PT, Miller KL, Glahn DC, Fox PM, Mackay CE, Filippini N, Watkins KE, Toro R, Laird AR, Beckmann CF (2009) Correspondence of the brain's functional architecture during activation and rest. Proc Natl Acad Sci 106 (31):13040–13045. https://doi.org/10.1073/pnas.0905267106

Solodkin A, Hlustik P, Chen EE, Small SL (2004) Fine modulation in network activation during motor execution and motor imagery. Cerebral cortex 14(11):1246–1255. https://doi.org/10.1093/cercor/bhh086

Sporns O (2014) Contributions and challenges for network models in cognitive neuroscience. Nat Neurosci 17(5):652–660. https://doi.org/10.1038/nn.3690

Tavor I, Parker Jones O, Mars RB, Smith SM, Behrens TE, Jbabdi S (2016) Task-free MRI predicts individual differences in brain activity during task performance. Science 352(6282):216–220. https://doi.org/10.1126/science.aad8127

Tsvetanov KA, Henson RN, Tyler LK, Razi A, Geerligs L, Ham TE, Rowe JB, Cambridge Centre for A, Neuroscience (2016) Extrinsic and intrinsic brain network connectivity maintains cognition across the lifespan despite accelerated decay of regional brain activation. J Neurosci 36(11):3115–3126. https://doi.org/10.1523/JNEUROSCI.2733-15.2016

Wang LB, Liu Q, Shen H, Li H, Hu DW (2015) Large-scale functional brain network changes in taxi drivers: evidence from resting state fMRI. Hum Brain Mapp 36(3):862–871. https://doi.org/10.1002/Hbm.22670

Woo CW, Chang LJ, Lindquist MA, Wager TD (2017) Building better biomarkers: brain models in translational neuroimaging. Nat Neurosci 20(3):365–377. https://doi.org/10.1038/nn.4478

Zabelina DL, Andrews-Hanna JR (2016) Dynamic network interactions supporting internally-oriented cognition. Curr Opin Neurobiol 40:86–93. https://doi.org/10.1016/j.conb.2016.06.014

Zhang T, Liu T, Li F, Li M, Liu D, Zhang R, He H, Li P, Gong J, Luo C, Yao D, Xu P (2016) Structural and functional correlates of motor imagery BCI performance: insights from the patterns of fronto-parietal attention network. NeuroImage 134:475–485. https://doi.org/10.1016/j.neuroimage.2016.04.030

Zhang Y, Wang Y, Jin J, Wang X (2017) Sparse Bayesian learning for obtaining sparsity of EEG frequency bands based feature vectors in motor imagery classification. Int J Neural Syst 27(02):1650032